NASA TN D-1492

NASA TN D-1492

TECHNICAL NOTE

D-1492

AN ANALYTICAL STUDY OF EFFECTS OF SOME AIRPLANE AND LANDING-GEAR FACTORS ON THE RESPONSE TO RUNWAY ROUGHNESS WITH APPLICATION TO SUPERSONIC TRANSPORTS

By Norman S. Silsby

Langley Research Center
Langley Station, Hampton, Va.

NATIONAL AERONAUTICS AND SPACE ADMINISTRATION

WASHINGTON December 1962

NATIONAL AERONAUTICS AND SPACE ADMINISTRATION

TECHNICAL NOTE D-1492

AN ANALYTICAL STUDY OF EFFECTS OF SOME AIRPLANE AND LANDING-GEAR FACTORS OF THE RESPONSE TO RUNWAY ROUGHNESS WITH APPLICATION TO SUPERSONIC TRANSPORTS

By Norman S. Silsby

SUMMARY

An analytical study has been made of the effects of several airplane and landing-gear design variables on the airplane response to runway roughness (for a relatively smooth runway) with application to supersonic transport configurations. Assumptions made for the analysis were (1) natural frequency of all tires were the same, (2) tires had no damping and possessed a linear tire-deflection load curve, (3) all struts had linear damping and spring characteristics, and the natural frequency and damping of all struts were the same, (4) rigid airplane structure, and (5) no aerodynamic forces.

The results of the analytical study indicated that, within the limitations of the assumptions made, the parameter variations considered had little effect on motions of the center of gravity of the airplane except for longitudinal position of the landing gear with respect to the center of gravity; in the latter case, moving the landing gear aft with respect to the center of gravity caused a reduction in center-of-gravity displacement and acceleration at all speeds. The effects of parameter changes on motions of the pilot's compartment were strongly influenced by speed; that is, changes which increased the response at one speed could cause decreased response at another speed. From the standpoint of root-mean-square accelerations at the pilot's compartment, placing the main gear near the center of gravity appeared to be advantageous; however, it resulted in somewhat higher displacements than with the main gear placed further rearward from the center of gravity. Generally, the supersonic transport configurations gave higher root-mean-square accelerations at the pilot's compartment than did a subsonic jet transport configuration.

INTRODUCTION

As presently envisaged, supersonic transports are expected to have an unusually long fuselage, a major portion of it extending forward of the center of gravity. This design will allow the possibility of landing-gear arrangements and locations relative to the pilot and passenger compartments substantially different from those of current aircraft. During take-offs and landings, these configurations may cause motions or accelerations undesirable for cockpit instruments, pilots, and/or passengers.

The present study was undertaken to examine the effects of such differences on the responses of the pilot's compartment and the airplane center of gravity due to runway roughness of a relatively smooth runway. The results are also compared with estimates for a current subsonic jet transport airplane.

SYMBOLS

a,b,c	constants
C	constant
C_s	strut damping coefficient
D	differential operator, d/dt
$D^* = D/a$	
F	input force from runway
g	acceleration due to gravity, 32.2 ft/sec^2
$i = \sqrt{-1}$	
k_s	strut spring constant
k_t	tire spring constant
k_y	pitch radius of gyration, ft
l	wheel base (nose gear to main gear), ft
l_m	distance from center of gravity to main gear, ft
l_n	distance from center of gravity to nose gear, ft
L	wavelength, ft
m	static mass on one gear
M	static mass on all wheels
s	distance along runway, ft
V	airplane speed along runway, ft/sec
x	longitudinal distance from center of gravity, positive forward, ft

X_o generalized output term

X_i generalized input term

z vertical displacement, ft

$$\alpha_{cg} = \frac{1 + \left(\frac{\omega_s}{\omega_t}\right)^2}{2\lambda_s \frac{\omega_s}{\omega_t}}$$

$$\alpha_\theta = \frac{1 + \left(\frac{\omega_s}{\omega_t}\right)^2}{2\lambda_s \frac{\omega_s}{\omega_t}\sqrt{\frac{l_m l_n}{k_y^2}}} = \frac{\alpha_{cg}}{\sqrt{\frac{l_m l_n}{k_y^2}}}$$

$$\beta_{cg} = \frac{\omega_s/\omega_t}{2\lambda_s}$$

$$\beta_\theta = \frac{\omega_s/\omega_t}{2\lambda_s\sqrt{\frac{l_m l_n}{k_y^2}}} = \frac{\beta_{cg}}{\sqrt{\frac{l_m l_n}{k_y^2}}}$$

θ pitch angle, radians

λ_s damping ratio of strut with static load mass

σ_z root-mean-square displacement, ft

$\sigma_{\ddot{z}}$ root-mean-square acceleration, g

σ_θ root-mean-square pitch angle, deg

ϕ phase angle, radians

$\Phi(\Omega)_r$ power-spectral-density function, sq ft/radian/ft

$\Phi(\Omega)_{\ddot{z}}$ power-spectral-density function, g^2/radian/ft

ω frequency, radians/sec

ω_s	natural frequency of strut with static load mass, 20 radians/sec
ω_t	natural frequency of tire with static load mass, 10 radians/sec
ω_θ	natural frequency of oscillation in pitch
ω^*	frequency ratio, ω/ω_t
Ω	spatial frequency, $2\pi/L$, radians/ft

Subscripts:

cg	center of gravity
i	input
l	refers to point between tire and strut
m	main gear
n	nose gear
θ	associated with oscillation in pitch
o	output
p	pilot compartment
r	runway
s	strut
t	tire
x	at x-position

Dots over symbols represent differentiation with respect to time. Bars over symbols denote vector quantities.

ASSUMPTIONS, ANALYSIS, AND METHOD OF EVALUATION

The following assumptions were made: (1) the natural frequency of the tires with the mass equivalent to the static load, was the same for the main and nose wheels, (2) the tires had no damping and possessed a linear tire-deflection-load curve, (3) all struts had linear damping and spring characteristics and the natural frequency and the damping of all the struts were the same, (4) the airplane fuselage was a rigid structure, and (5) there were no aerodynamic forces.

The equations of motion of the airplane resulting from forces applied to the tires as the airplane moved along the runway were derived under the assumptions stated. The resulting frequency response was combined with the power spectrum of runway roughness for a good runway $\Phi(\Omega)_r = \frac{6.7 \times 10^{-6}}{\Omega^2}$ (see ref. 1) to give the power spectrum of acceleration at various points along the airplane longitudinal axis resulting from center-of-gravity translations and pitching responses. The root-mean-square accelerations, displacements, and pitch angles were determined by integrating these spectra over the range of wavelengths from 4 feet to 570 feet. The computations were carried out by using a digital computer for 50 points in this range for each of the 7 discrete speeds of 40, 80, 120, 160, 200, 240, and 280 feet per second. A complete development of the equations used in the analysis is presented in the appendix. Figure 1 defines the dimensional symbols representing the characteristics of the airplane.

The parameters which were varied were landing-gear wheel base l, longitudinal location of the landing gear with respect to the center of gravity, and radius of gyration k_Y. Responses were calculated for various points along the longitudinal axis.

The long slender fuselage envisaged for the supersonic transport may be more flexible than those of current jet transports. The acceleration responses for such a fuselage may be somewhat different from those presented herein for an assumed rigid fuselage, depending on such factors as the modes excited, their natural frequencies, arrangement of the landing gear, airplane speed, and so forth.

Presentation of Results

The results of the analytical study are presented in figures 2 to 4. Table I shows the airplane configurations, values of the parameters used, and the figure numbers in which these various configurations appear. Figure 2 shows the variation with velocity of the root-mean-square values of normal accelerations, the root-mean-square normal displacements, and the root-mean-square pitch angles due to the variation of the landing-gear location with respect to the center of gravity (fig. 2(a)), the variation of the pitching radius of gyration (fig. 2(b)), and the variation of the length of the landing-gear wheel base (fig. 2(c)). Figure 3 shows the variations of root-mean-square accelerations and displacements with location along the longitudinal axis for various speeds for a possible supersonic transport configuration having a short wheel base (45 ft) relative to overall length (fig. 3(a)) and for a 90-foot wheel base (fig. 3(b)). Figure 4 compares the variation with velocity of the same quantities shown in figure 2 for the supersonic transport and a current subsonic turbojet transport calculated by the same method.

DISCUSSION

Effect of Landing-Gear Location

The effect of varying the longitudinal location of the landing gear with respect to the center of gravity so that the main gear varied from $0.1l$ to $0.3l$ aft of the center of gravity (fig. 2(a)) is to reduce the root-mean-square displacements and accelerations of the center of gravity at all speeds. The root-mean-square acceleration at the pilot's compartment nearly doubled at the higher speeds as the landing gear was moved aft; however, the maximum acceleration was only about 0.3g and this was for a relatively smooth runway. From the standpoint of root-mean-square accelerations at the pilot's compartment, placing the main gear near the center of gravity appeared to be advantageous; however, it resulted in somewhat higher displacements (0.3-foot maximum) than with the main gear placed further rearward from the center of gravity (about 0.2-foot maximum displacement). The root-mean-square pitch angles were less than 0.2° for all these gear locations and showed no important variations with speed.

Effect of Pitching Radius of Gyration

As would be expected, changing the radius of gyration in pitch had no effect on the values of root-mean-square accelerations and displacements at the center of gravity. Halving the pitching radius of gyration from 28.3 feet ($k_y/l = 0.63$) to 14.15 feet ($k_y/l = 0.315$) resulted in a threefold increase in root-mean-square accelerations at the pilot's compartment at the higher speeds, with the maximum value about 0.45g. (See fig. 2(b).)

At a speed of 240 feet per second it may be noted that, for the pilot's compartment, although the values of the displacements and the pitch angles are about equal for the various configurations, there is a substantial variation in the values of root-mean-square accelerations. The reason, at least in part, is probably the difference in the natural frequency in pitch of the configurations. The values of root-mean-square accelerations should be proportional to the square of the natural frequencies since the displacements are essentially the same.

Effect of Length of Landing-Gear Wheel Base

Increasing the length of the landing-gear wheel base (by moving the nose wheel forward) while also maintaining a constant pitch radius of gyration showed that substantial reductions could be realized in both root-mean-square pitching angles and root-mean-square displacements for the pilot's compartment over almost the entire range of velocities. (See fig. 2(c).) For example, doubling the wheel base from 45 feet to 90 feet results in a reduction of root-mean-square displacements by a factor of as much as 6 at a velocity of about 120 feet per second and a reduction of root-mean-square pitch angle by a factor of about 5 for the same speed. Increasing the landing-gear wheel base had mixed effects on accelerations, depending on speed. Although the intermediate wheel-base length (67.5 feet) yielded values of root-mean-square pitch angles and displacements which fell generally between those for the 45- and 90-foot wheel bases, this intermediate wheel-base length produced the greatest root-mean-square accelerations at speeds above 120 feet per second.

Variation With Distance Along the Fuselage

For the configuration with a wheel base of 45 feet (fig. 3(a)), the values of displacement and acceleration response at speeds of 40, 80, 120, and 160 feet per second appear to be a minimum at or near the center of gravity and exhibit a fairly smooth and uniform increase in the values with increasing distance either toward the nose or tail at all speeds. For the configuration with a wheel base of 90 feet, however (fig. 3(b)), the minimum values of displacements and accelerations occur at points somewhat displaced from the center of gravity ($x/l = 0$) for all speeds (in this figure, 40, 80, 160, and 240 ft/sec). For a speed of 40 feet per second the minimum acceleration was near the center of gravity; at 80 feet per second the minimum response was toward the tail ($x/l = -0.4$); and for speeds of 160 and 240 feet per second the minimum response locations were toward the nose ($x/l \approx 0.5$).

Comparison of Hypothetical Supersonic Transport Configuration

With Current Subsonic Jet Transport

The curves of figure 4 indicate that, for the pilot's compartment for the 45-foot wheel base, the root-mean-square displacements of the supersonic transport were greater than those for the subsonic transport by factors from $1\frac{1}{2}$ to $2\frac{1}{2}$ over the speed range. However, for the 90-foot wheel-base supersonic transport, the displacements were about the same or somewhat lower than those for the subsonic transport. The root-mean-square acceleration and pitch angles for the supersonic transport (45-foot wheel base) were up to 50 percent larger than those for the subsonic transport. For the 90-foot wheel-base configuration, the pitch angles were lower than those for the subsonic transport over the entire speed range; however, the root-mean-square accelerations were higher than those for the subsonic transport at the lowest and highest speeds and about the same in the mid-speed range (110 to 180 ft/sec).

CONCLUDING REMARKS

A simplified analysis has been made to examine certain design variables of landing-gear location and aircraft pitch radius of gyration in relation to possible effects on the response of supersonic transport configurations to runway roughness. The results indicate that the parameter variations considered had little effect on motions of the center of gravity of the airplane except for longitudinal position of the landing gear with respect to the center of gravity; moving the landing gear aft resulted in a reduction in center-of-gravity displacement and acceleration at all speeds. The effects of the parameter changes on the motions of the pilot's compartment were strongly influenced by speed; that is, changes which increased the response at one speed could cause decreased response at another speed. From the standpoint of root-mean-square accelerations at the pilot's compartment, placing the main gear near the center of gravity appeared to be advantageous; however, it resulted in somewhat higher displacements than with the main gear placed further rearward from the center of gravity.

Increasing the pitching radius of gyration tended to reduce the root-mean-square accelerations and increase displacements at the pilot's compartment. Increasing the landing-gear wheel base tended to decrease pilot's compartment displacement response but had mixed effects on accelerations, depending on speed.

The highest accelerations were obtained with an intermediate wheel base of 67.5 feet in a range from 45 feet to 90 feet at speeds above 120 feet per second.

Generally, the supersonic transport configurations gave higher root-mean-square accelerations at the pilot's compartment than did a subsonic jet transport configuration.

Langley Research Center,
National Aeronautics and Space Administration,
Langley Station, Hampton, Va., August 2, 1962.

APPENDIX

THEORETICAL ANALYSIS

Determination of Acceleration Response of the Airplane Due to Runway Roughness

The following assumptions are considered in this analysis. For each wheel, the static load is considered to be rated static load, and for this condition the natural frequency on all tires ω_t is assumed to be the same. In addition, the strut response is assumed to be linear, and all struts have the same frequency responses and damping ratios (with static load on given wheel as a separate mass and neglecting mass of wheels and struts).

Determination of the Transfer Function for the Center-of-Gravity Translation and Pitching of the Airplane

With reference to figure 1 the following equations may be written:

$$F = k_t\left(z_i - z_1\right) = k_s\left(z_1 - z_o\right) + C_s\left(\dot{z}_1 - \dot{z}_o\right) \tag{1}$$

The equations of motion in vertical translation are:

$$M\ddot{z}_{cg_o} = F_n + F_m = k_{t_n}\left(z_i - z_1\right)_n + k_{t_m}\left(z_i - z_1\right)_m \tag{2}$$

Since $m_n = \frac{l_m}{l}M$ and $m_m = \frac{l_n}{l}M$,

$$M\ddot{z}_{cg_o} = \frac{k_{t_n}}{m_n}\frac{l_m}{l}M\left(z_i - z_1\right)_n + \frac{k_{t_m}}{m_m}\frac{l_n}{l}M\left(z_i - z_1\right)_m \tag{3}$$

If $\frac{k_{t_n}}{m_n} = \frac{k_{t_m}}{m_m} = \omega_t^2$, then

$$\ddot{z}_{cg_o} = \omega_t^2\left[\frac{l_m}{l}\left(z_i - z_1\right)_n + \frac{l_n}{l}\left(z_i - z_1\right)_m\right] \tag{4}$$

Also

$$M\ddot{z}_{cg_o} = k_{s_n}\left(z_1 - z_o\right)_n + C_{s_n}\left(\dot{z}_1 - \dot{z}_o\right)_n + k_{s_m}\left(z_1 - z_o\right)_m + C_{s_m}\left(\dot{z}_1 - \dot{z}_o\right)_m \tag{5}$$

or

$$\begin{aligned} M\ddot{z}_{cg_o} &= \frac{k_{s_n}}{m_n}\frac{l_m}{l}M\left(z_1 - z_o\right)_n + \frac{C_{s_n}}{m_n}\frac{l_m}{l}M\left(\dot{z}_1 - \dot{z}_o\right)_n \\ &\quad + \frac{k_{s_m}}{m_n}\frac{l_n}{l}M\left(z_1 - z_o\right)_m + \frac{C_{s_m}}{m_n}\frac{l_n}{l}M\left(\dot{z}_1 - \dot{z}_o\right)_m \end{aligned} \tag{6}$$

If $\dfrac{k_{s_n}}{m_n} = \dfrac{k_{s_m}}{m_m} = \omega_s^2$ and $\dfrac{C_{s_n}}{m_n} = \dfrac{C_{s_m}}{m_m} = 2\lambda_s\omega_s$, then

$$\begin{aligned} \ddot{z}_{cg_o} &= \omega_s^2\frac{l_m}{l}\left(z_1 - z_o\right)_n + 2\lambda_s\omega_s\frac{l_m}{l}\left(\dot{z}_1 - \dot{z}_o\right)_n \\ &\quad + \omega_s^2\frac{l_n}{l}\left(z_1 - z_o\right)_m + 2\lambda_s\omega_s\frac{l_n}{l}\left(\dot{z}_1 - \dot{z}_o\right)_m \end{aligned} \tag{7}$$

The following relation also may be written:

$$z_{cg_{i,1,o}} = \frac{l_m}{l}z_{n_{i,1,o}} + \frac{l_n}{l}z_{m_{i,1,o}} \tag{8}$$

Substituting equation (8) into equations (4) and (7) yields

$$\ddot{z}_{cg_o} = \omega_t^2\left(z_i - z_1\right)_{cg} \tag{9}$$

and

$$\ddot{z}_{cg_o} = \omega_s^2\left(z_1 - z_o\right)_{cg} + 2\lambda_s\omega_s\left(\dot{z}_1 - \dot{z}_o\right)_{cg} \tag{10}$$

The equation of motion in pitch is

$$Mk_y^2\ddot{\theta}_o = x_nF_n - x_mF_m \tag{11}$$

Substituting the expressions for F_n and F_m from equation (2) into equation (11), together with the equations for m_n, m_m, and ω_t^2, yields

$$Mk_y^2\ddot{\theta}_o = M\frac{l_m l_n}{l}\omega_t^2\left(z_i - z_1\right)_n - M\frac{l_m l_n}{l}\omega_t^2\left(z_i - z_1\right)_m \tag{12}$$

From figure 1, $\theta_{i,1,o} = \frac{z_n - z_m}{l}$ and $\dot{\theta}_{i,1,o} = \frac{\dot{z}_n - \dot{z}_m}{l}$. Therefore,

$$\ddot{\theta}_o = \frac{l_m l_n}{k_y^2}\omega_t^2\left(\theta_i - \theta_1\right) \tag{13}$$

Also

$$Mk_y^2\ddot{\theta}_o = M\frac{l_m l_n}{l}\omega_s^2\left(z_1 - z_o\right)_n - \left(z_1 - z_o\right)_m$$

$$+ 2M\frac{l_m l_n}{l}\lambda_s\omega_s\left(\dot{z}_1 - \dot{z}_o\right)_n - \left(\dot{z}_1 - \dot{z}_o\right)_m \tag{14}$$

or

$$\ddot{\theta}_o = \frac{l_m l_n}{k_y^2}\omega_s^2\left(\theta_1 - \theta_o\right) + 2\frac{l_m l_n}{k_y^2}\lambda_s\omega_s\left(\dot{\theta}_1 - \dot{\theta}_o\right) \tag{15}$$

The solution of equations (9), (10), (13), and (15) yields the transfer functions for the center-of-gravity translation and pitching responses of the airplane to runway inputs. Equations (9) and (13) are of the form

$$\ddot{X}_o = a^2\left(X_i - X_1\right) \tag{16}$$

and equations (10) and (15) are of the form

$$\ddot{X}_o = b^2\left(X_1 - X_o\right) + c\left(\dot{X}_1 - \dot{X}_o\right) \tag{17}$$

where a, b, and c are constants, and X_i is the displacement of the runway undulations or the input, and X_o is the resulting displacement of the airplane or the output. X_1 is the displacement relating to motions of the wheel axles and lower parts of the shock struts. Writing equations (16) and (17) in operator form and rearranging results in the following:

$$D^2X_o + a^2X_1 = a^2X_i \tag{18}$$

$$\left(D^2 + cD + b^2\right)X_o - \left(cD + b^2\right)X_1 = 0 \tag{19}$$

Equations (18) and (19) can be evaluated simultaneously by eliminating X_1 to obtain

$$\left[D^3 + \left(\frac{a^2 + b^2}{c}\right)D^2 + a^2D + \frac{a^2b^2}{c}\right]X_o = \left(a^2D + \frac{a^2b^2}{c}\right)X_i \tag{20}$$

Taking $D = aD^*$ and rewriting equation (20) yields the nondimensional form:

$$\left[D^{*3} + \frac{1 + (b/a)^2}{c/a}D^{*2} + D^* + \frac{(b/a)^2}{c/a}\right]X_o = \left[D^* + \frac{(b/a)^2}{c/a}\right]X_i \tag{21}$$

or

$$\left(D^{*3} + \alpha D^{*2} + D^* + \beta\right)X_o = \left(D^* + \beta\right)X_i \tag{22}$$

where

$$\alpha = \frac{1 + (b/a)^2}{c/a} \tag{23}$$

and

$$\beta = \frac{(b/a)^2}{c/a} \tag{24}$$

From equation (22) the response ratio is obtained:

$$\frac{\overline{X}_o}{\overline{X}_i} = \frac{\sqrt{\left[\beta\left(\beta - \alpha\omega^{*2}\right) + \omega^{*2}\left(1 - \omega^{*2}\right)\right]^2 + \left[(\alpha - \beta)\omega^{*3}\right]^2}}{\left(\beta - \alpha\omega^{*2}\right)^2 + \omega^{*2}\left(1 - \omega^{*2}\right)^2} \tag{25}$$

where $\dfrac{\bar{x}_o}{\bar{x}_i} = \dfrac{\bar{z}_{cg_o}}{\bar{z}_{cg_i}}$ or $\dfrac{\bar{\theta}_o}{\bar{\theta}_i}$ and the phase angle between output and input:

$$\left(\phi_o - \phi_i\right) = \sin^{-1} \frac{-(\alpha - \beta)\omega^{*3}}{\sqrt{\left[\beta\left(\beta - \alpha\omega^{*2}\right) + \omega^{*2}\left(1 - \omega^{*2}\right)\right]^2 + \left[(\alpha - \beta)\omega^{*3}\right]^2}} \tag{26}$$

where

$$\omega_{cg}^* = \omega/\omega_t$$

$$\alpha_{cg} = \frac{1 + \left(\omega_s/\omega_t\right)^2}{2\lambda_s\left(\omega_s/\omega_t\right)}$$

$$\beta_{cg} = \frac{\omega_s/\omega_t}{2\lambda_s}$$

and

$$(\alpha,\beta,\omega^*)_\theta = (\alpha,\beta,\omega^*)_{cg}\sqrt{\frac{k_y^2}{l_m l_n}}$$

The next step is to determine the input information z_{cg_i} and θ_i in terms of the runway characteristics. If it is assumed that the runway roughness spectrum is made up of sinusoidal waves of spatial frequencies Ω and the runway displacement at the nose wheel is taken as reference, the input motion at the nose wheel for unit amplitude is

$$z_{n_i} = \bar{z}_{n_i} e^{i\Omega s} \tag{27}$$

where s is distance along the runway and the input at the main wheels is

$$z_{m_i} = \bar{z}_{n_i} e^{i\Omega(s-l)} \tag{28}$$

The displacement at the center of gravity resulting from displacements at the nose and main wheels is

$$z_{cg_i} = \frac{l_m}{l} z_{n_i} + \frac{l_n}{l} z_{m_i} \tag{29}$$

or

$$\frac{z_{cg_i}}{\bar{z}_{n_i}} = \left(\frac{l_m}{l} + \frac{l_n}{l} e^{-i\Omega l}\right) e^{i\Omega s}$$

from which

$$\frac{\bar{z}_{cg_i}}{\bar{z}_{n_i}} = \frac{\bar{z}_{cg_i}}{\bar{z}_r} = \sqrt{1 - \frac{2 l_m l_n}{l^2}(1 - \cos \Omega l)} \tag{30}$$

and the phase angle is

$$\phi_{cg_i} = \sin^{-1} \frac{\frac{-l_n}{l} \sin \Omega l}{\sqrt{1 - \frac{2 l_m l_n}{l^2}(1 - \cos \Omega l)}} \tag{31}$$

The pitch-angle displacement input is

$$\theta_i l = z_{n_i} - z_{m_i} \tag{32}$$

so that, from equations (27) and (28),

$$\frac{\theta_i l}{\bar{z}_{n_i}} = \left(1 - e^{-i\Omega l}\right) e^{i\Omega s} \tag{33}$$

from which

$$\frac{\bar{\theta}_i l}{\bar{z}_{n_i}} = \frac{\bar{\theta}_i l}{\bar{z}_r} = \sqrt{2(1 - \cos \Omega l)} \tag{34}$$

and the phase angle is

$$\phi_{\theta_i} = \sin^{-1} \frac{\sin \Omega l}{\sqrt{2(1 - \cos \Omega l)}}$$

or

$$\phi_{\theta_i} = \frac{1}{2}(\pi - \Omega l) \tag{35}$$

Equations (27) to (35) can be transformed to the time domain by the relation $\Omega = \omega/V$.

The phase angles of the aircraft motion relative to the runway displacement can then be determined from equations (26), (31), and (35) as

$$\phi_{o_{cg,\theta}} = \left(\phi_o - \phi_i\right)_{cg,\theta} + \phi_{i_{cg,\theta}} \tag{36}$$

The motion of the airplane at any distance x from the center of gravity along the x-axis where x is positive forward is then given by

$$\frac{z_{x_o}}{\bar{z}_r} = \frac{z_{cg_o}}{\bar{z}_r} + \frac{x}{l}\,\frac{l\theta_o}{\bar{z}_r} \tag{37}$$

or

$$\frac{z_{x_o}}{\bar{z}_r} = \frac{\bar{z}_{cg_o}}{\bar{z}_r}e^{i\phi_{cg_o}} + \frac{x}{l}\,\frac{l\bar{\theta}_o}{\bar{z}_r}e^{i\phi_{\theta_o}} \tag{38}$$

The response ratio at x is then given by

$$\frac{\bar{z}_{x_o}}{\bar{z}_r} = \sqrt{\left(\frac{\bar{z}_{cg_o}}{\bar{z}_r}\right)^2 + \left(\frac{x}{l}\,\frac{\bar{\theta}_o l}{\bar{z}_r}\right)^2 + 2\frac{\bar{z}_{cg_o}}{\bar{z}_r}\,\frac{x}{l}\,\frac{l\bar{\theta}_o}{\bar{z}_r}\cos\left(\phi_{cg_o} - \phi_{\theta_o}\right)} \tag{39}$$

The acceleration response at any point along the x-axis is then

$$\frac{\ddot{\bar{z}}_{x_o}}{\bar{z}_r} = \omega^2\,\frac{\bar{z}_{x_o}}{\bar{z}_r} \tag{40}$$

The power spectral density of airplane vertical acceleration in response to runway roughness is

$$\Phi(\Omega)_{\ddot{z}} = \left(\frac{\ddot{\bar{z}}_{x_o}}{\bar{z}_r}\right)^2\Phi(\Omega)_r \tag{41}$$

where the runway roughness spectrum was taken according to reference 1 to be

$$\Phi(\Omega)_r = \frac{C}{\Omega^2} = C\frac{V^2}{\omega^2} \tag{42}$$

with the value of $C = 6.7 \times 10^{-6}$ representing a good runway, used for the computations.

The root-mean-square acceleration $\sigma_{\ddot{z}}$ at various points along the x-axis of the airplane were obtained from the relation

$$\sigma_{\ddot{z}}^2 = \int_{\frac{2\pi}{L_o}}^{\frac{2\pi}{L_f}} \Phi_{\ddot{z}}\, d\Omega = \frac{1}{V}\int_{\frac{2\pi V}{L_o}}^{\frac{2\pi V}{L_f}} \Phi_{\ddot{z}}\, d\omega$$

For the speeds considered in the analysis and considering the frequency-response characteristics of the airplane there appeared to be little power in the airplane-acceleration response spectrum for runway wavelengths greater than 570 feet; L_o was therefore given this value. For the upper limit of the integration, the wavelength L_f was taken as 4 feet because runway roughness measurements do not ordinarily go below this value.

REFERENCE

1. Houbolt, John C.: Runway Roughness Studies in the Aeronautical Field. Jour. Air Transport Div., Proc. American Soc. Civil Eng., vol. 87, no. AT 1, Mar. 1961, pp. 11-31.

TABLE I.- VALUES OF PARAMETERS USED IN ANALYSIS

l, ft	l_m/l	l_n/l	k_y/l	k_y	ω_θ, radians/sec	Figure
Supersonic configuration						
45	0.1	0.9	0.63	28.3	4.28	2(a), 2(b), 2(c), 4
45	.2	.8	.63	28.3	5.72	2(a)
45	.3	.7	.63	28.3	6.62	2(a)
45	.1	.9	.50	22.5	5.40	2(b), 3(a)
45	.1	.9	.315	14.15	8.76	2(b)
45	.1	.9	.50	22.5	5.40	3(a)
45	.1	.9	.50	22.5	5.40	3(a)
45	.1	.9	.50	22.5	5.40	3(a)
45	.1	.9	.50	22.5	5.40	3(a)
67.5	.1	.9	.419	28.3	6.50	2(c)
90	.1	.9	.315	28.3	8.76	3(b)
90	.1	.9	.315	28.3	8.76	3(b)
90	.1	.9	.315	28.3	8.76	3(b)
90	.1	.9	.315	28.3	8.76	2(c), 3(b)
90	.1	.9	.315	28.3	8.76	3(b)
Subsonic jet transport						
52.33	.1	.9	.50	26.16	5.40	4

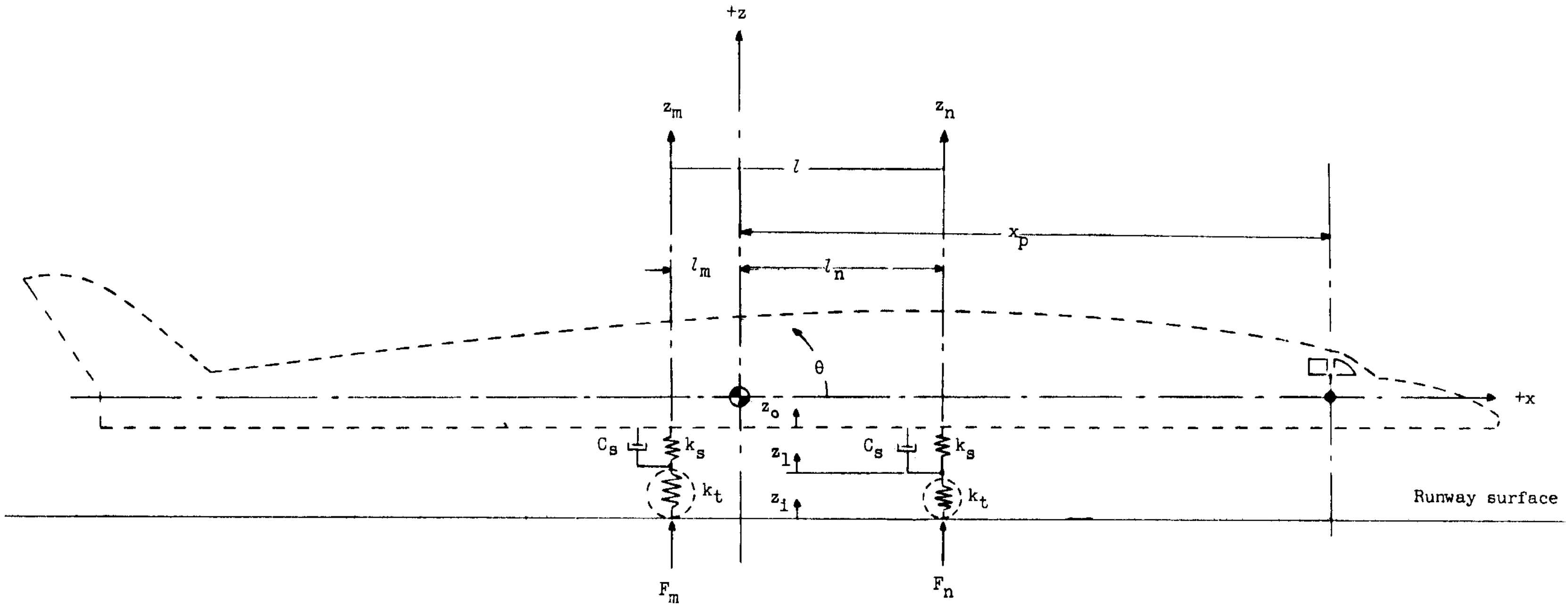

Figure 1.- Sketch defining dimensional symbols for analysis.

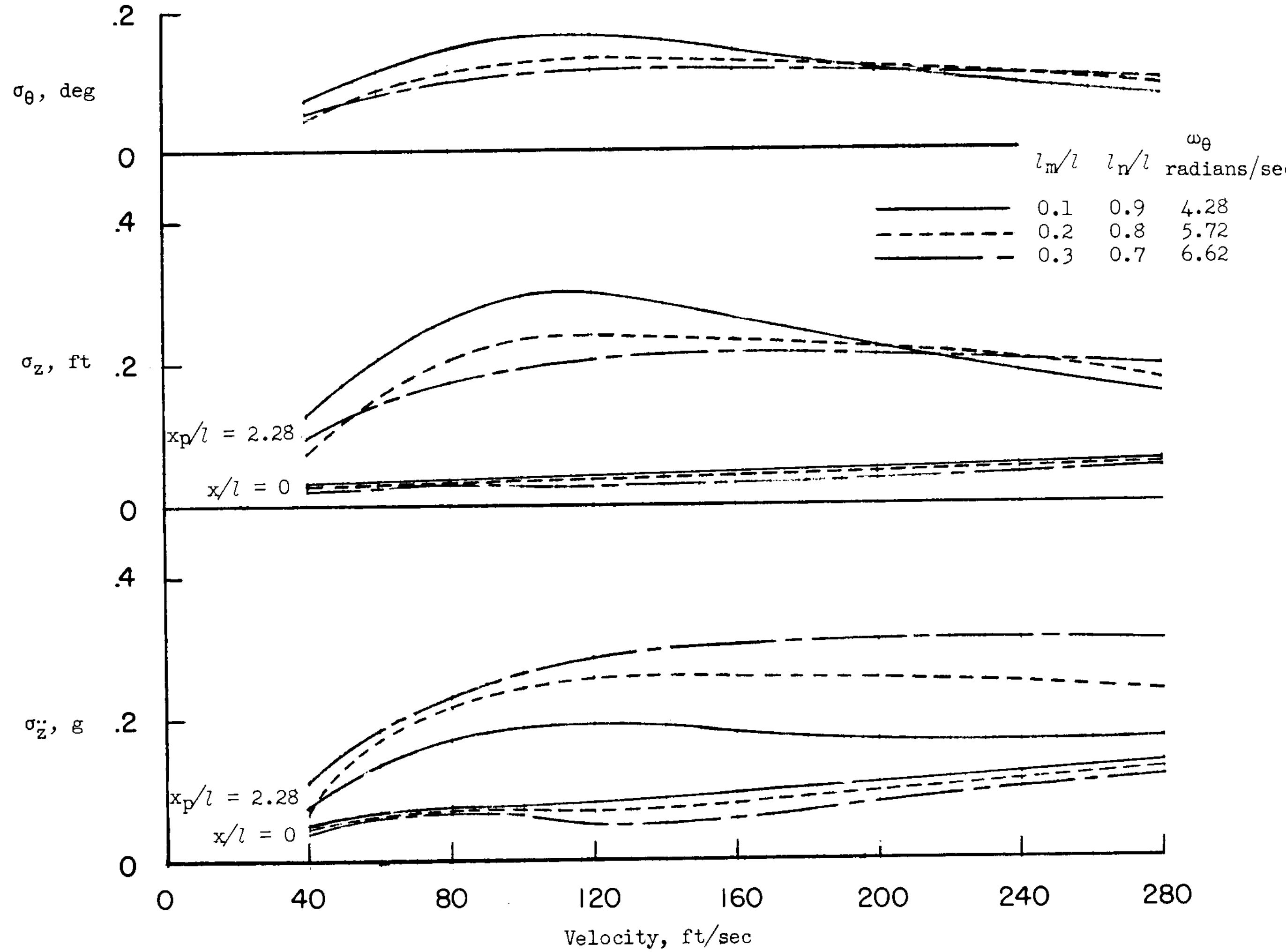

(a) Effect of landing-gear location with respect to the center of gravity $\left(l_m/l,\ l_n/l\right)$. l = 45 feet; k_y/l = 0.63.

Figure 2.- Variation with speed of the root-mean-square values of normal acceleration and normal displacement at the center of gravity and at the pilot's compartment of a supersonic transport configuration. Root-mean-square values of pitch angle are also shown.

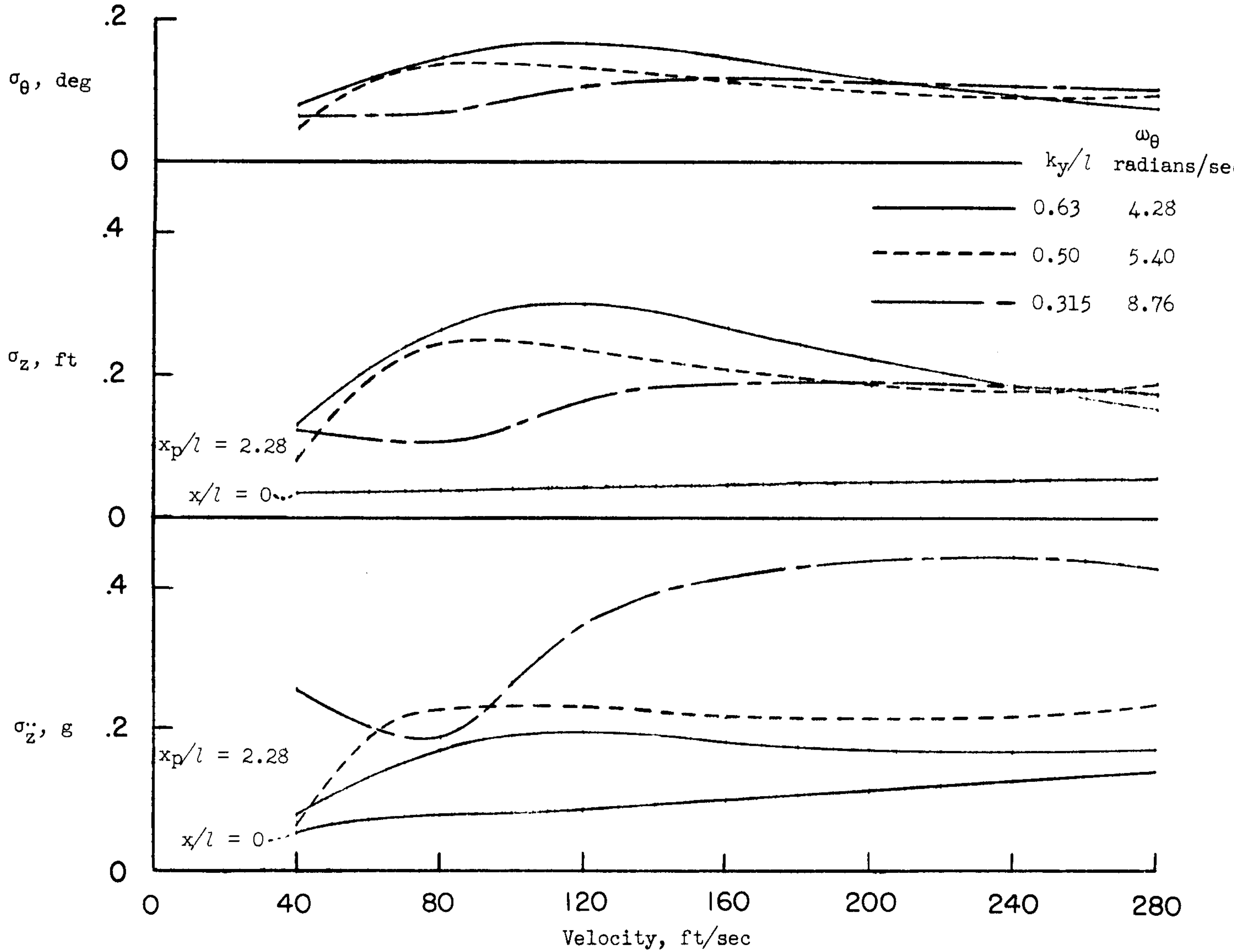

(b) Effect of variation of pitching radius of gyration $\left(k_y/l\right)$.
l = 45 feet; l_m/l = 0.1; l_n/l = 0.9.

Figure 2.- Continued.

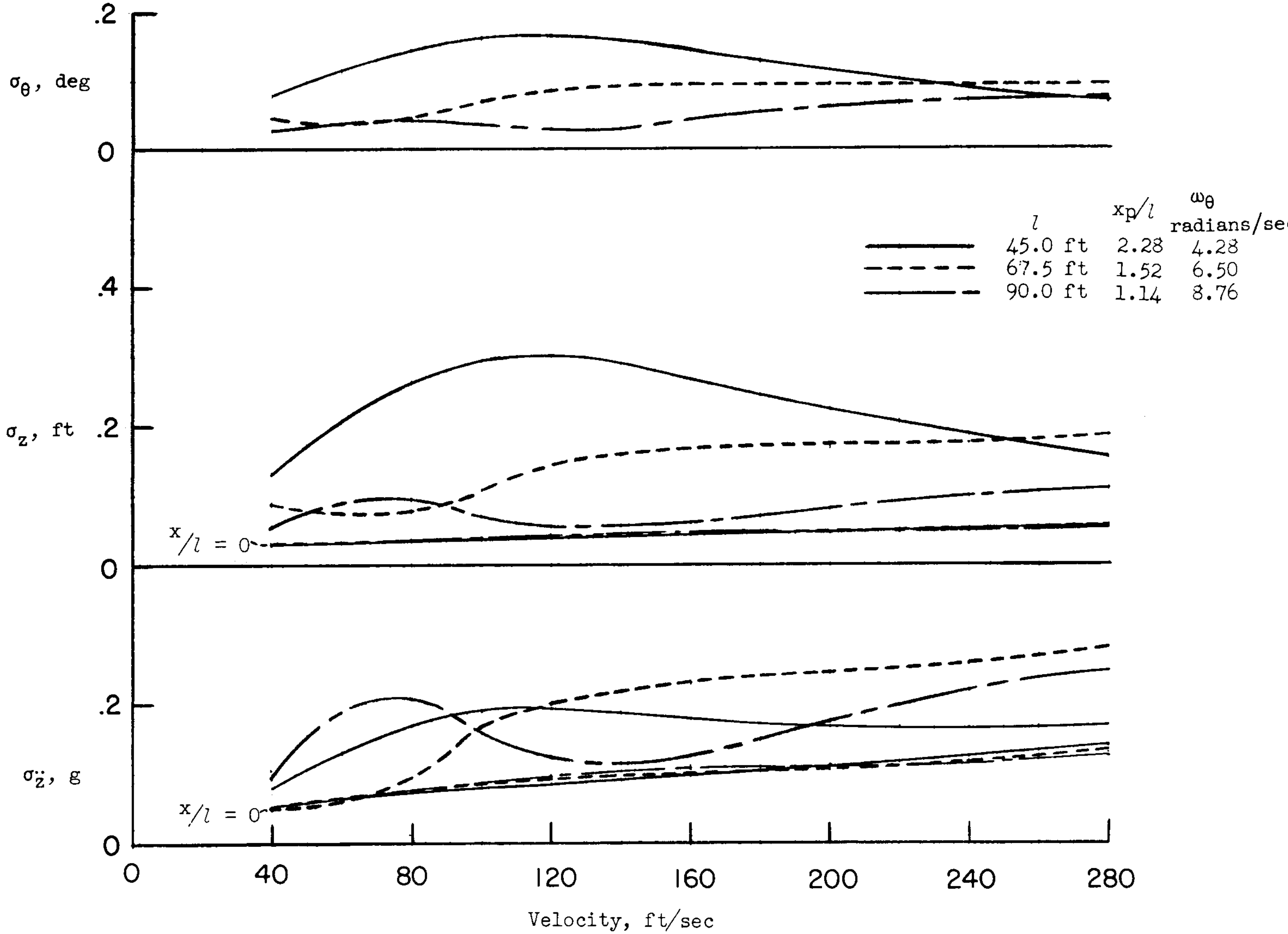

(c) Effect of variation of length of landing-gear wheel base, l. $l_m/l = 0.1$; $l_n/l = 0.9$; $k_y = 28.3$ feet.

Figure 2.- Concluded.

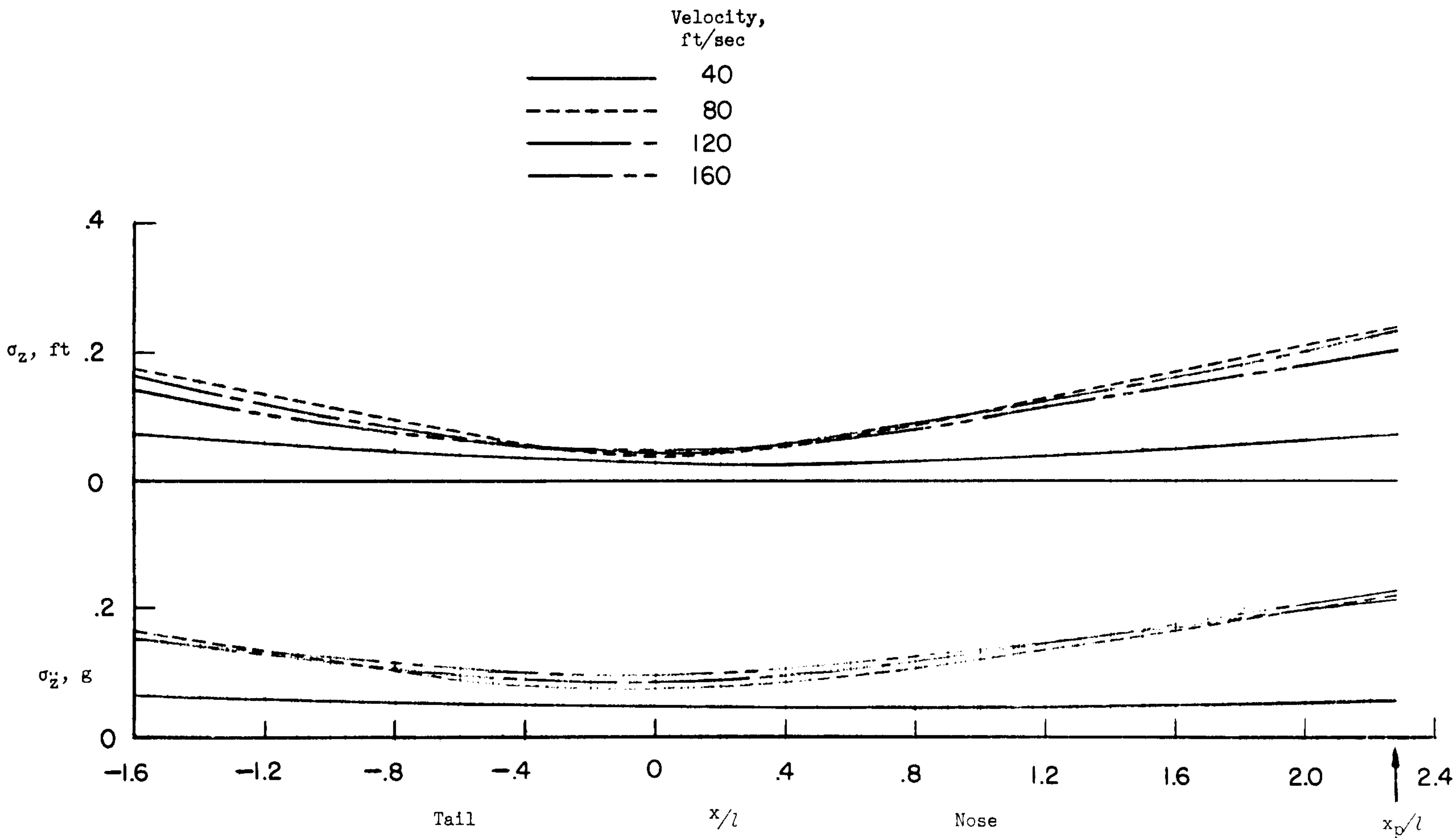

(a) l = 45 feet; k_y/l = 0.50; k_y = 22.5 feet.

Figure 3.- Variation of root-mean-square normal acceleration and normal displacement with location along the longitudinal axis of a supersonic airplane configuration for various speeds. $l_m/l = 0.1$; $l_n/l = 0.9$.

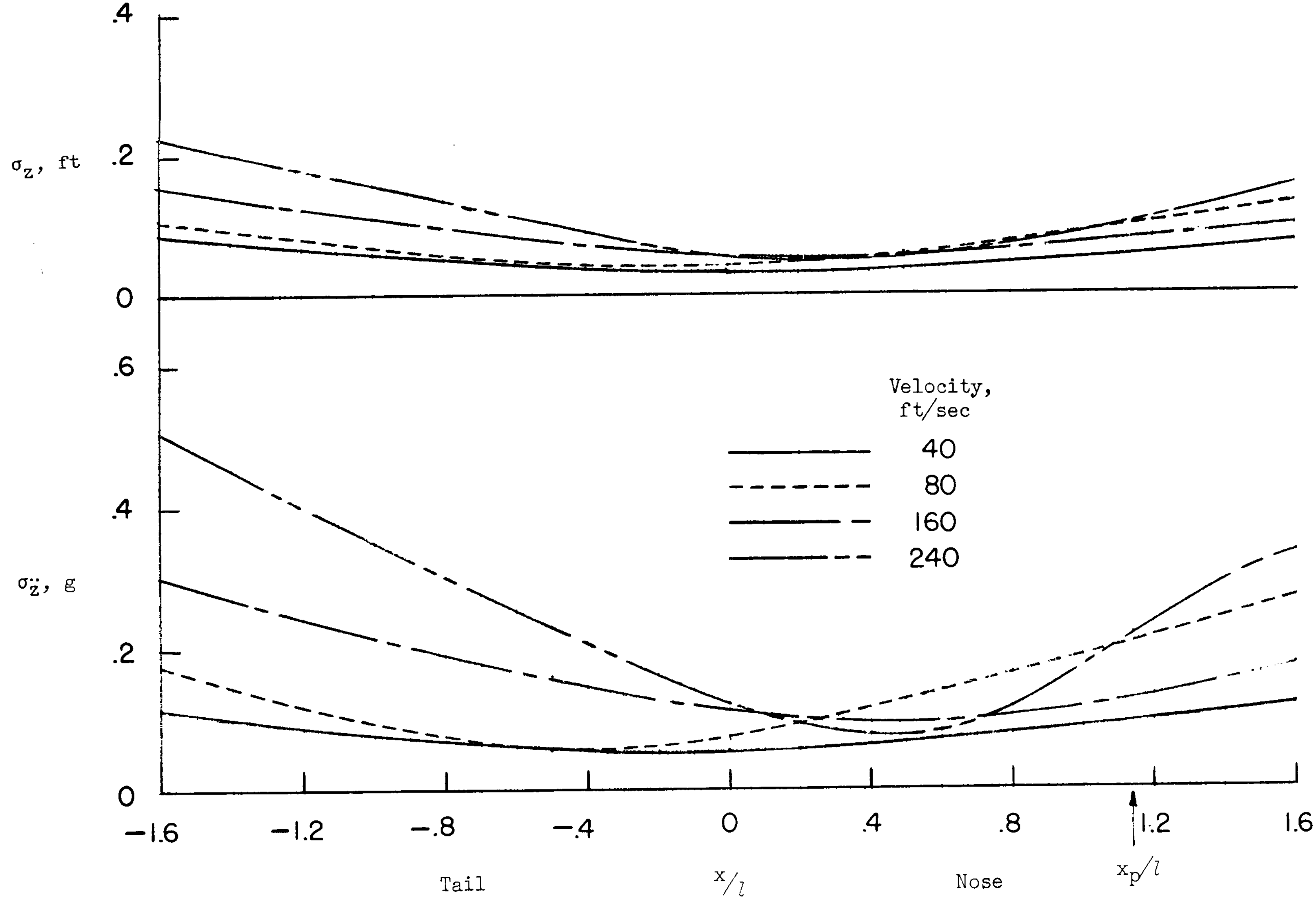

(b) l = 90 feet; k_y/l = 0.315; k_y = 28.3 feet.

Figure 3.- Concluded.

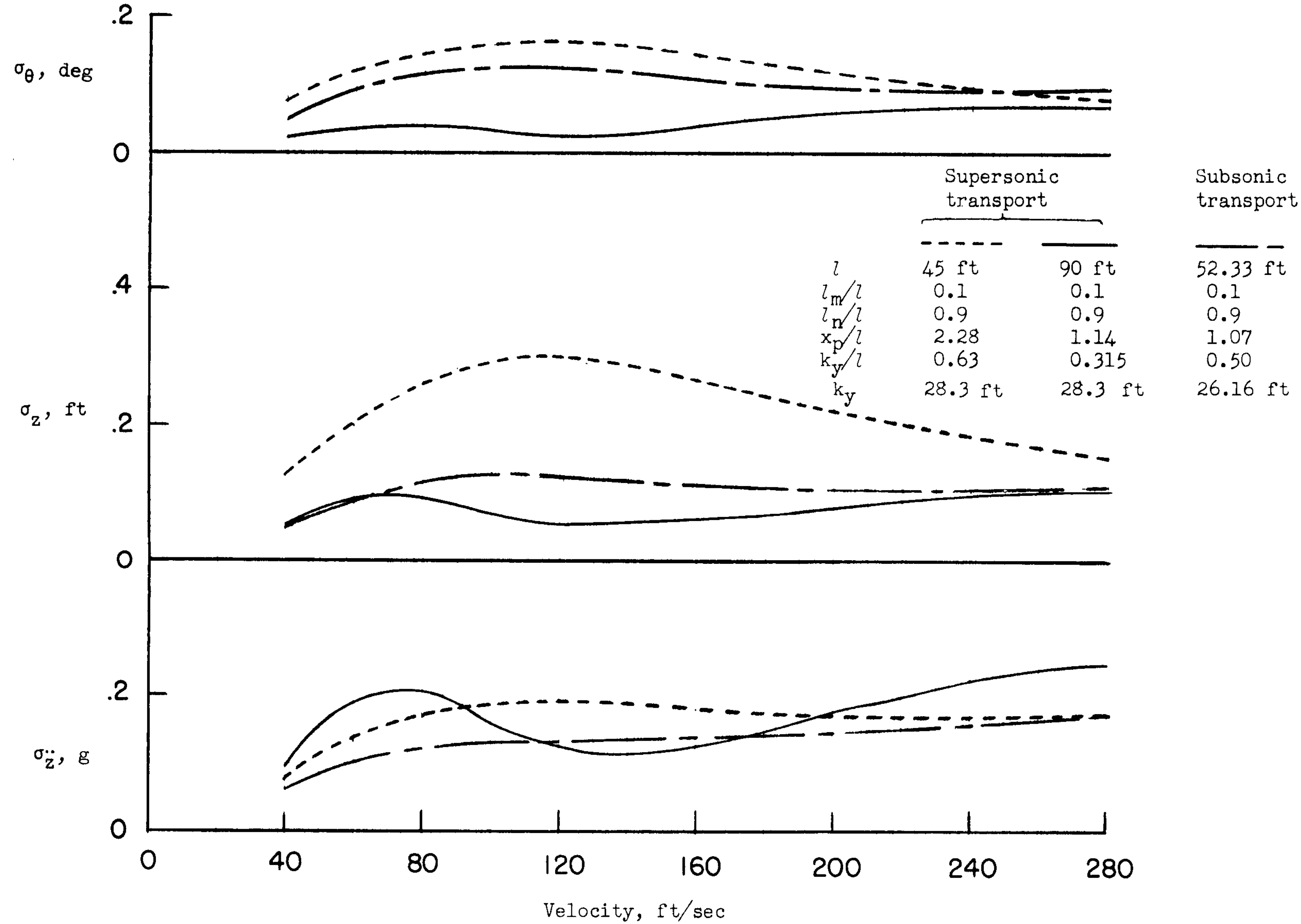

Figure 4.- Comparison of the variation with velocity of the root-mean-square values of normal acceleration, normal displacement, and pitch angle for a current subsonic turbojet transport and a supersonic transport configuration.